Sol–Gel Methods for the Assembly of Metal Chalcogenide Quantum Dots

INDIKA U. ARACHCHIGE AND
STEPHANIE L. BROCK*
Department of Chemistry, Wayne State University, Detroit, Michigan 48202

Received December 13, 2006

ABSTRACT
Sol–gel chemistry represents a powerful method for assembling metal chalcogenide quantum dots into 3D connected architectures without the presence of intervening ligands to moderate particle–particle interactions. Wet gels prepared by the oxidative loss of thiolate surface groups from chalcogenide nanoparticles can be converted to xerogels (low porosity) or aerogels (high porosity), and the quantum-confinement effects in these low-dimensional networks decrease with increasing density of the network. In this Account, we describe the application of sol–gel chemistry to the formation of CdSe architectures and discuss how surface modification can lead to highly luminous monoliths, concluding with the prospects of these unique materials for applications in sensing and photovoltaics.

Introduction

Quantum dots (semiconducting nanoparticles) have the potential to revolutionize many traditional and emerging technologies, including solar-energy conversion, biological imaging, and data processing and recording, owing to their unique optoelectronic properties.[1–4] In particular, quantum dots exhibit size-tunable optical absorption thresholds and narrow and intense photoluminescence spectral features that are resistant to photobleaching.[5] The distinctive "quantum-confinement effects" of semiconductor nanoparticles arise from the fact that there are insufficient atoms to generate the continuum of energy levels that are characteristic of the valence and conduction bands in a bulk semiconductor material; a series of discrete "atom-like" states is present instead. Thus, the energy difference between the filled and empty levels depends upon the number of atoms. That is, below some critical radius, the Bohr radius of the electron–hole pair (exciton), the effective "band gap" increases as the particle size decreases. While this critical radius is material-dependent, typical values for semiconductors range from a few nanometers to a few tens of nanometers.[6]

The interest in quantum dot properties has sparked a sustained research effort to develop synthetic methods that permit exquisite control over size, shape, and polydispersity. Considerable progress has been made over the past decade, such that several classes of quantum dots, among them metal chalcogenide nanoparticles, can be easily synthesized in high quantity and quality.[7,8] However, many of the envisioned applications or devices are not based on single nanocrystals or solutions of nanocrystals but are predicated on the formation of nanoparticle assemblies in the solid state. Methodologies for bottom–up assembly of nanoparticles into functional architectures have not been extensively studied. Two common approaches that have been exploited include the formation of nanoparticle superlattices and glassy films by controlled solvent evaporation[9–13] and the use of organic transformations on nanoparticle surface groups to effect cross-linking between particles.[14–16] However, in each of these cases, the interactions between particles are mediated by surface ligands, the presence of which are detrimental to electrical transport properties and limit thermal stability.

In point of fact, we have at our disposal a tried-and-true method for constructing nanoparticle assemblies from nanoparticle building blocks *without* the presence of intervening ligands: sol–gel chemistry. Over the past 75 years (and starting long before the term "nano" became the buzzword that it is today), the sol–gel method has been widely exploited for creating nanostructures of SiO_2, Al_2O_3, TiO_2, V_2O_5, and SnO_2, among others.[17–19] Traditional oxide-based sol–gel reactions include a series of hydrolysis and condensation reactions in which the nanoparticles (colloidal sols) are formed from molecular precursors and aggregated to form a wet gel network. Dependent upon how the wet gel is dried, the density and extent of porosity in the network can be effectively tuned, consequently impacting the bulk physical properties. The low dimensionality of the framework and the presence of an interconnected pore space have been exploited for a range of applications, including thermal/acoustic insulation, catalysis, and battery or sensor devices.[20] However, sol–gel methods have been largely "oxocentric", limiting the chemical diversity and hence the range of material properties that can be accessed. In particular, there is a distinct advantage in moving from oxides to sulfides, selenides, and tellurides because of the increased covalency (and decreased band gap) in the semiconducting phases. Specifically, chalcogenide semiconductors, such as CdS, CdSe, and CdTe, are absorbers in the visible-to-infrared (IR) region, and the characteristics of the absorp-

Indika Arachchige was born in Kegalle, Sri Lanka, in 1975 and received his B.S. degree in chemistry from the University of Kelaniya, Sri Lanka, in 2001. He is currently a Wiligred Heller Graduate Fellow in the Department of Chemistry at Wayne State University. His doctoral research is focused on the sol–gel assembly of metal chalcogenide nanoparticles and is performed under the direction of Professor Brock.

Stephanie Brock was born in Alameda, CA, in 1967. She obtained her B.S. degree in chemistry from the University of Washington in 1990 and her Ph.D. degree in chemistry from the University of California at Davis in 1995 (under the direction of Professor Susan Kauzlarich). After postdoctoral study in chemistry under the direction of Professor Steven Suib at the University of Connecticut, she joined Wayne State University in 1999, where she is currently an Associate Professor of Chemistry. Her honors include a Research Corporation Research Innovation Award and a NSF–CAREER award. Her research interests lie in the synthesis, properties, and applications of metal pnictide and chalcogenide extended solids and nanomaterials, sol–gel methods for nanoparticle assembly, and organic–inorganic hybrid materials for biomedical applications.

* To whom correspondence should be addressed. E-mail: sbrock@chem.wayne.edu.

10.1021/ar600028s CCC: $37.00
Published on Web 04/19/2007

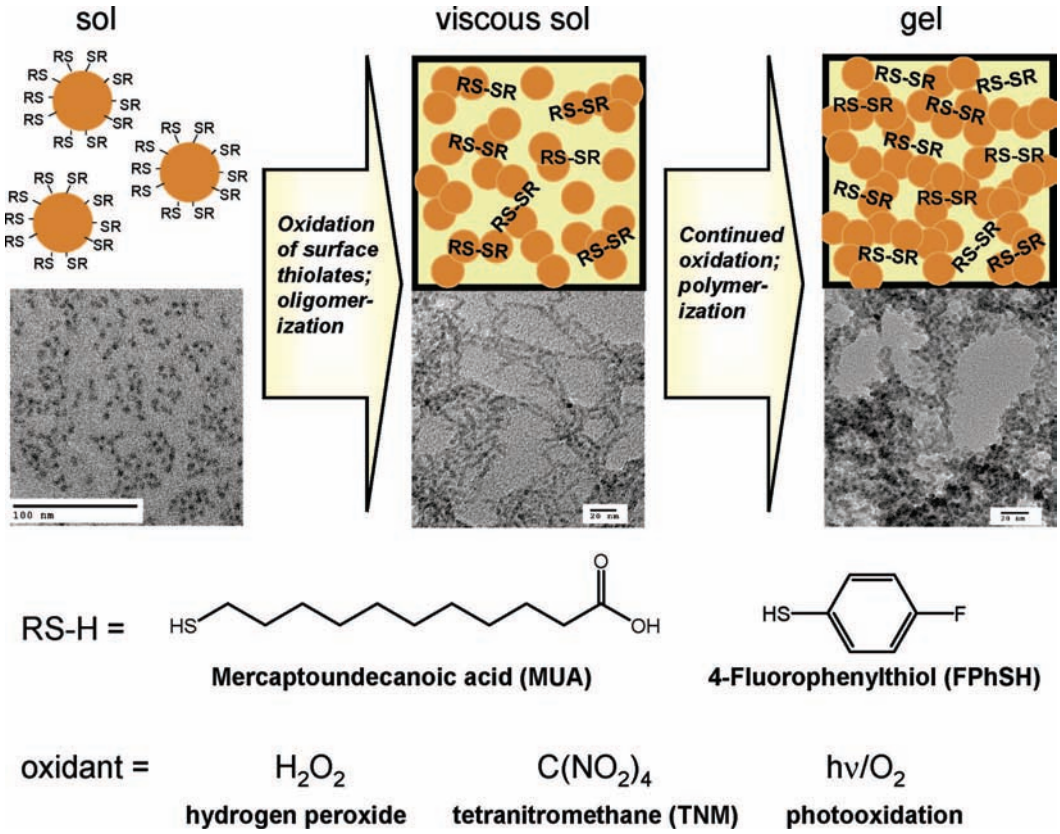

FIGURE 1. Scheme and associated transmission electron microscopy (TEM) micrographs showing the gel formation, via a viscous sol, of metal chalcogenide nanoparticles that are surface-capped with thiolates (RS^-). Upon introduction of an oxidant, disulfides are formed (RS–SR), providing open sites on the particle surface for assembly into oligomers and eventually polymers (gels). Representative thiols (RS–H) and oxidants are also illustrated. The micrographs are of CdSe materials [prepared with ca. 3 nm spherical particles using MUA for capping and tetranitromethane (TNM) for oxidation], with the bar corresponding to 100, 20, and 20 nm, respectively, from left to right.

tion and emission profile can be adjusted by controlling the particle size, whereas TiO_2 or SnO_2 require sensitization/doping to absorb at visible wavelengths. Thus, developing sol–gel methods for linking together chalcogenide nanoparticles can be expected to lead to electrically connected device architectures for diverse applications, including photovoltaics and sensors. Furthermore, gel structures provide a platform for evaluating how the architecture of a 3D connected network of nanoparticles impacts quantum-confinement effects.

The limited studies that have been performed on chalcogenide sol–gel chemistry by thiolysis and nanoparticle assembly routes have been recently reviewed.[21] Thus, in the present work, we will focus on new results from our lab on CdSe nanoparticle assembly and surface modification for improved photoluminescence properties. The role of dimensionality on quantum confinement will be discussed along with the potential of such materials for future applications.

Sol–Gel Transition for Metal Chalcogenide Quantum Dots

The oxidation-induced loss of thiolate groups from metal chalcogenide nanoparticle surfaces, originally reported by Gacoin and coworkers for CdS,[22–26] is a versatile method for transforming nanoparticle sols to chalcogenide gels (Figure 1). This methodology is applicable to a range of metal chalcogenides, including ZnS, CdS, CdSe, and PbS.[21,27–31] The formed gels are colloidal in nature, similar to silica gels prepared under base-catalyzed conditions,[19] a consequence of the fact that they arise from the linkage of preformed spherical nanoparticles. The metal chalcogenide nanoparticle precursors can be prepared from a range of well-established methodologies, although we have focused on arrested precipitation reactions conducted in water-in-oil microemulsions (inverse micelles) at room temperature or high-temperature methods conducted in coordinating solvents.[8,32] These approaches are illustrated in Figure 2 for the case of CdSe. The as-prepared nanoparticles are either stabilized by electrostatic interactions between surface Cd^{2+} species and the anionic sodium bis(2-ethylhexyl)sulfosuccinate (AOT) surfactant or dative bonds between Cd and the P═O functionality of trioctylphosphine oxide (TOPO). The chalcophilicity of Cd drives the displacement of these ligands by thiolates upon treatment with thiol [e.g., mercaptoundecanoic acid (MUA) or FPhS] under basic conditions.

The treatment of thiolate-capped metal chalcogenide nanoparticles with an appropriate oxidant (we have successfully employed H_2O_2, TNM, and $h\nu/O_2$) results in the oxidation of the thiolate (RS^-) to a radical ($RS^\bullet$), followed by a combination of the alkylthiyl radicals to

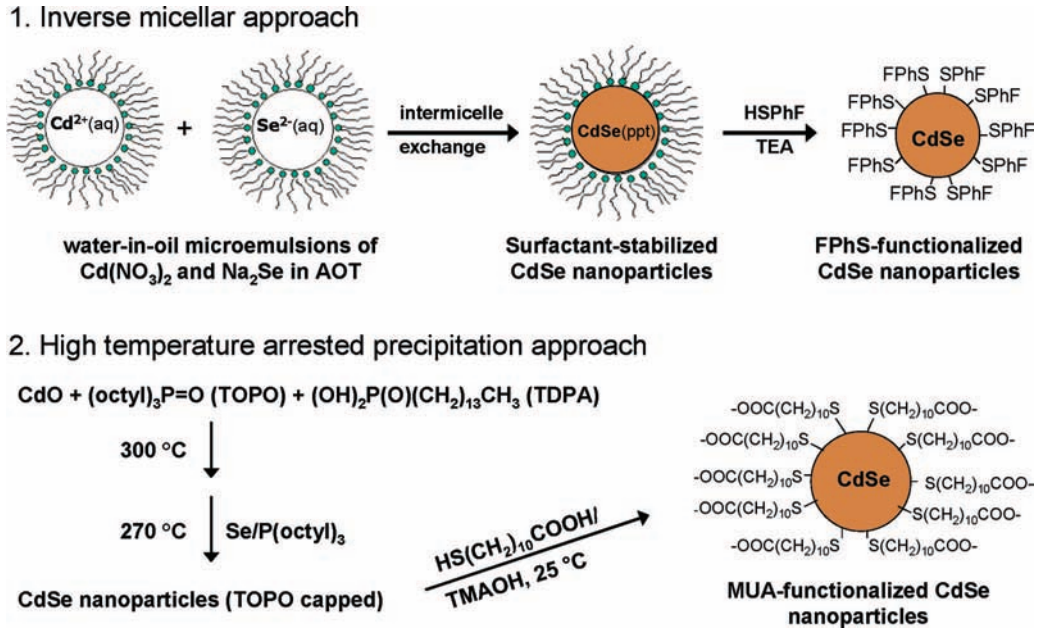

FIGURE 2. Schemes showing the inverse-micellar and high-temperature arrested precipitation approaches for nanoparticle synthesis, as applied to the case of CdSe, and the surface functionalization with thiolate. The water-in-oil microemulsion employs sodium bis(2-ethylhexyl)sulfosuccinate (AOT) as the surfactant, with water as a minority phase in heptane. The treatment with triethylamine (TEA) and 4-fluorophenylthiol (FPhSH) yields thiolate-capped CdSe nanoparticles that demonstrate high solubility in acetone. High-temperature methods employ coordinating solvents to limit particle growth, in this case trioctylphosphine oxide (TOPO) and tetradecylphosphonic acid (TDPA). Thiolate capping is achieved by treatment with MUA and tetramethylammonium hydroxide (TMAOH), yielding particles with excellent solubility in water and alcohols. More details can be found in ref 27.

form disulfides (RS–SR) as the primary byproduct. H_2O_2 and TNM are sufficiently reactive to oxidize the thiolates without assistance. In contrast, oxidation by O_2 requires initial photoexcitation of the quantum dot. O_2 traps the excited electron in the conduction band, and the hole left in the valence band then reacts with the thiolate.[33] The efficiency of the oxidation process governs how quickly the sol–gel transition occurs, by controlling the availability of reactive sites on the particle surface. The ability to transform a colloidal solution of nanoparticles (sol) to a solvent-swollen polymeric network (gel) relies in part on the kinetics by which active sites for assembly become available on the particle surface. If no sites are available because of strict passivation of the particle surface, the colloid is stable, whereas if too many sites become available at any one time, precipitation can occur. This can be tuned by altering the quantity of oxidant relative to the amount of thiolate present or the chemical reactivity of the oxidant. Thus, at some minimum ratio of oxidant/thiolate, X_{min}, no gel is formed.[23] Above X_{min}, the rapidity at which gel formation occurs increases with increasing X, until the kinetics are so fast that a precipitate forms in lieu of a gel at $\sim 5X_{min}$. Likewise, photo-oxidation of MUA-capped CdSe nanoparticles in air leads to gelation over a timeframe of days to weeks under ambient lighting,[27,29] where the reactivity of oxygen is low, but direct irradiation at 254 nm with an ultraviolet (UV) lamp results in precipitation within hours.[33]

The density of the resultant gels is also a sensitive function of the oxidant concentration, as well as the aging time. At high concentrations of the oxidant, the large number of surface reactive sites facilitates interparticle linkages, resulting in a more compact gel. Likewise, continued polymerization during the aging process leads to densification of the monoliths, as illustrated in Figure 3 for CdSe. Importantly, it has been shown that the use of a large excess of oxidant and/or long aging times leads to complete removal of thiolate from CdS nanoparticles; thus, the interparticle linkages can be presumed to be purely inorganic in nature.[25] In practice, unless very dense gels are sought, lower oxidant concentrations/shorter aging times are employed and some degree of residual thiolate remains in the samples.

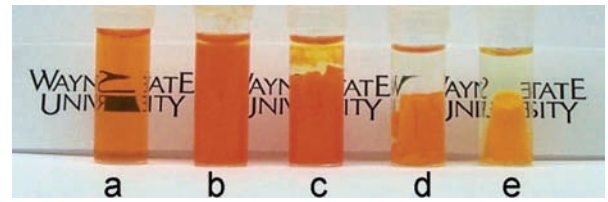

FIGURE 3. Photographs illustrating the transformation of the transparent CdSe sol to an opaque gel and the compaction and syneresis (solvent expulsion) that occurs upon aging the gel: (a) sol, (b) viscous sol, 35 min after the addition of the oxidant, (c) gel aged 6 days, (d) gel aged 3 weeks, and (e) gel aged 3 months. Gelation was achieved by adding 0.025 mL of TNM into 2 mL of a 0.25 M (on the basis of the original Cd concentration in the high-temperature nanoparticle synthesis) CdSe sol.

Removing the Solvent: Xerogel and Aerogel Formation

As can be seen from Figure 3, the wet gel is a continuously evolving structure, owing to the ease of species migration through the liquid medium. Additionally, many of the

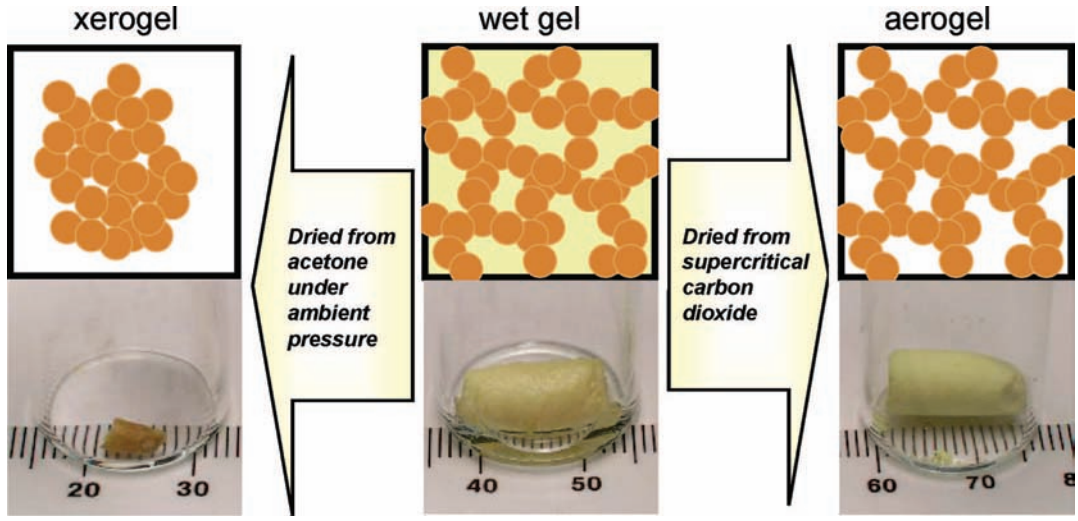

FIGURE 4. Scheme and associated photographs showing the acetone-saturated wet gel, the xerogel formed from ambient-pressure drying, and the aerogel prepared from supercritical CO_2 drying. Capillary forces result in pore collapse in the xerogel; the absence of a liquid–gas interface in the supercritical solvent removes surface tension, allowing for the solvent to be removed without significantly impacting the wet gel structure, resulting in an aerogel. The photographs are of CdS materials and are reprinted with permission from ref 29. Remarkably, the aerogel has a bulk density of 0.07 g/cm^3, which is <2% of that of a CdS single crystal.

device applications envisioned for nanoparticle assemblies are predicated on solid-state structures. Solvent removal is thus a critical step for stabilizing the microstructure and creating architectures with desired functionality that are compatible with existing device structures.

The metal chalcogenide gel structure itself is, however, a direct consequence of the solvent. The solvent acts as a template to support the spanning aggregates. Consequently, the removal of the solvent can have a huge impact on the gel structure.[17] When solvents capable of wetting the pore walls of the gel (i.e., of similar polarity) are evaporated under ambient pressure conditions or vacuum, capillary forces arise in the pores because of the liquid–vapor interface, inducing pore collapse and, consequently, densification. As can be seen for the case of a CdS gel in Figure 4, the resulting xerogels occupy a fraction of the volume of the wet gel, having lost a considerable amount of their porosity. One way to maintain the wet gel structure while removing the solvent is to use supercritical solvents, because there can be no liquid–vapor interface and, consequently, capillary forces. This methodology was originally reported by Kistler in 1931, who surmised that it should be generally applicable to a wide range of gels.[34,35] Indeed, our data (Figure 4) suggest that the colloidal metal chalcogenide gels can be transformed to aerogels by evaporation of supercritical CO_2 at ca. 40 °C. Even more impressive is the fact that metal chalcogenide gels can be formed as monoliths. Among the oxides, only a few systems (silica, alumina, etc.) have gels that can be transformed to monolithic aerogels.[36–40] For many materials that will undergo gelation, the network is simply not robust enough to remain an interconnected whole during the drying process, although this can be alleviated by polymer encapsulation.[41]

The consequences of drying on the microstructure of the gel network are reflected in the surface area and pore-size distributions, as probed by nitrogen adsorption/desorption isotherms (see Figure 5). The adsorption/desorption isotherms obtained for the CdSe aerogels are similar in shape, regardless of the methodology used to synthesize the primary nanoparticles, and resemble a type IV curve with a sharp upturn in the high relative pressure region similar to a type II curve. This sharp upturn or lack of saturation in the high relative pressure region is indicative of liquid condensation associated with the presence of large (macroscopic, >50 nm) pores in the aerogels. The hysteresis loop of the adsorption/desorption isotherm of the aerogel is similar in both types of aerogels and has a combination of H1 and H3 characters that correspond to cylindrical and slit shape pore geometries, respectively. The adsorption/desorption isotherms of CdSe xerogels also correspond to a type IV curve, indicating mesoporosity, but in contrast to the aerogels, the hysteresis loops observed in the xerogel isotherm correspond to a H2-type loop, indicative of "ink-bottle neck" shaped pores in a dense network.[42,43] Overall, CdSe xerogels have 25–50% of the available surface area of corresponding aerogels, and the distribution of pore sizes as a function of the pore volume is much narrower, with an average size of 4–5 nm for the xerogel relative to 16–29 nm for the aerogel. Thus, the cumulative pore volume for the xerogels is on the order of 10% of that for aerogels. However, this process of aggregation and drying has very little effect on the nanocrystalline properties of the building blocks. Powder X-ray diffraction analysis of low-temperature-prepared CdSe particles and their associated aerogels and xerogels is characteristic of a cubic polymorph, whereas high-temperature-prepared materials are hexagonal. For either synthesis, the peaks have a considerable breadth associated with the short coherence length in the nanoparticles. Only a slight increase (<10%) in crystallite size is observed because of aggregation (i.e., gel formation).

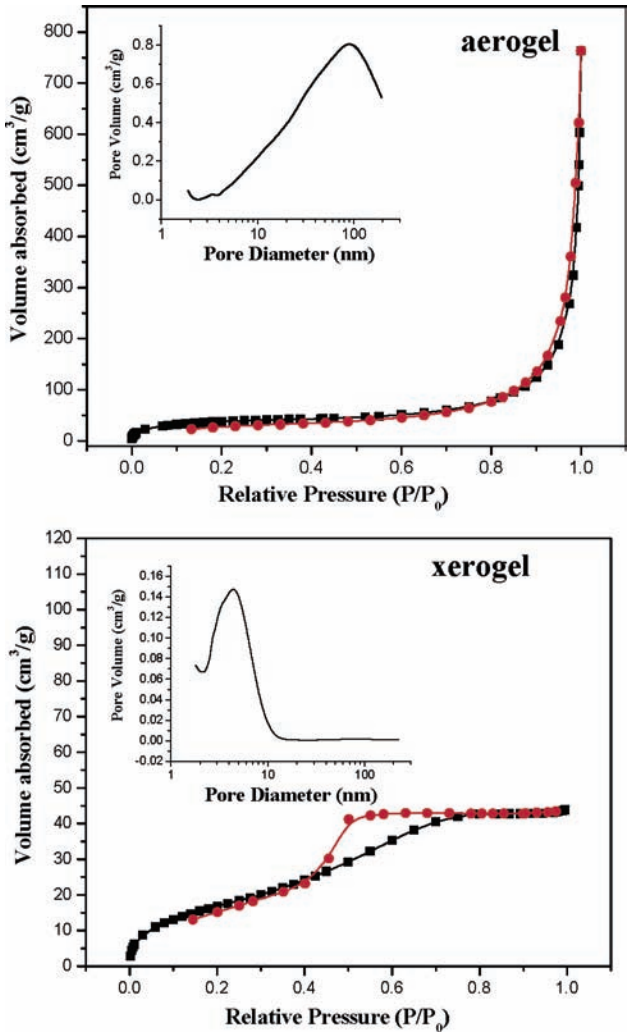

FIGURE 5. Representative nitrogen adsorption–desorption isotherms and Barrett–Joyner–Halenda (BJH) plots of the pore size versus volume (insets) of a CdSe aerogel and xerogel synthesized from inverse-micelle-prepared nanoparticles. The dramatic increase in density for the xerogel, illustrated in Figure 4, translates to a significant decrease in the available surface area and pore size relative to the supercritically dried aerogel. The Brunauer–Emmett–Teller (BET) surface area for the aerogel = 128–161 m^2/g, and the BET surface area for the xerogel = 41–65 m^2/g.[27,28] Xerogel plots were reproduced with permission from ref 28. Copyright 2005 American Chemical Society

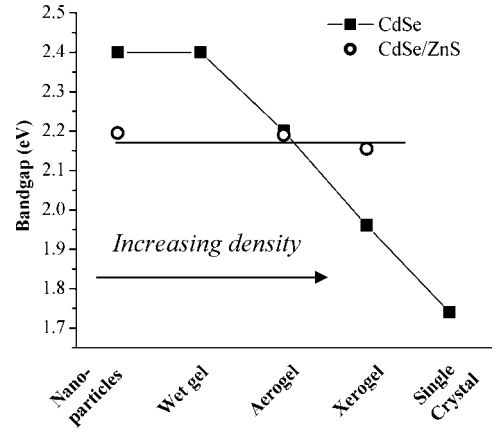

FIGURE 6. Illustration of the effect of the network density on the optical properties of gel structures composed of naked CdSe quantum dots and ZnS-capped CdSe quantum dots (CdSe/ZnS). The optical band gap of materials in the naked CdSe system decreases as the density increases. This can be ascribed to a decrease in the extent of quantum confinement as the dimensionality of the architecture increases from 0D (nanoparticles) to 3D (large single crystals). For the analogous case of CdSe/ZnS, CdSe remains 0D because of the ZnS shell. Thus, network densification has little effect on the optical band gap.

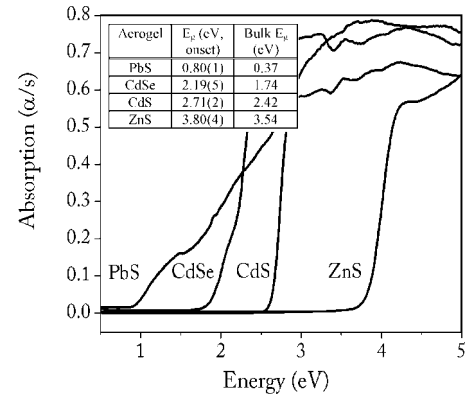

FIGURE 7. Diffuse reflectance data for aerogels of PbS, CdSe, CdS, and ZnS and the corresponding band gap values for bulk crystalline samples. In each case, the optical band gap for the aerogel is significantly blue-shifted from that of the bulk, suggesting that the quantum-confinement effects of the nanoparticles are retained within the 3D-linked aerogel architecture. This figure was reprinted with permission from ref 29.

Optical Properties of Nanostructured Gels and Consequences for Quantum Confinement

Despite the fact that the gel network consists of a 3D connected architecture of quantum dots without the presence of intervening ligands, the size-dependent optical band gap of the CdSe wet gels is essentially identical to those of the precursor nanoparticles (Figure 6). The aerogel shows a red shift in the band edge relative to the precursor nanoparticles/wet gels, and the xerogels continue the trend (Figure 6). Nevertheless, all are consistent with some degree of quantum confinement; i.e., all exhibit a blue shift relative to the value for a bulk single crystal. Additionally, this is not unique to CdSe but is observed in all of the systems that we have investigated to date (Figure 7).[28,29] How is it that such large (~1 cm) interconnected monoliths behave like particles with critical diameters of 6 orders of magnitude smaller?

It is well-established that quantum-confinement effects can be retained in materials that have dimensions less than the excitonic Bohr radius in at least one direction.[44] The extent of confinement depends upon the number of degrees of freedom or dimensionality (D); thus, quantum dots (0D) are more confined than quantum rods ($0 < D < 1$), which in turn are more confined than quantum wires (1D) and wells (2D).[45–48] Gel networks actually have a fractal or intermediate dimensionality because of the porosity.[49] Thus, although particles are connected in 3D, they are unique structures inherently different from bulk

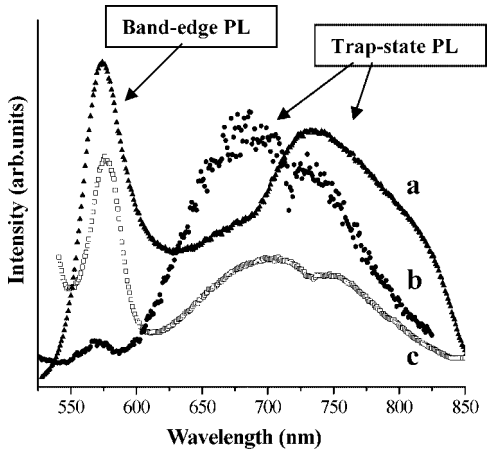

FIGURE 8. Photoluminescence spectra of (a) high-temperature-prepared CdSe nanoparticles, (b) aerogels prepared from CO_2 supercritical drying of wet gels exchanged with acetone, and (c) aerogels prepared from CO_2 supercritical drying of wet gels exchanged several times with pyridine and then exchanged with acetone. The pyridine displaces some of the residual surface thiolate functionalities in the wet gel, resulting in an increase in the intensity of the band-edge luminescence peak relative to the trap-state peak. This figure was reproduced with permission from ref 27. Copyright 2006 American Chemical Society.

crystals. At a local level, the degree of interaction (number of particles) is much lower than in a bulk solid of uniform density.

If this should be the case, one would expect that the extent of quantum confinement would depend upon the density of the network, such that higher density networks would be a closer approximation to the bulk solids. As indicated in Figure 6, this is exactly what we see. The more dense xerogel structure is less quantum-confined (smaller band gap) than the aerogel. Therefore, the extent of quantum confinement in metal chalcogenide gel networks is ultimately related to the dimensionality (density) of the network.

Upping the Luminosity through Surface Modification

The photoluminescence properties of metal chalcogenide nanomaterials are strongly dependent upon crystallinity and surface characteristics.[50,51] The presence of defects gives rise to midgap states where electron–hole recombination can occur, thereby reducing the band-edge luminescence properties and giving rise to a broad, red feature in the emission spectrum. It is well-established that certain ligands act as strong quenching agents for the band-edge luminescence, thiolates among them, by acting as hole acceptors.[52] Thus, even highly crystalline hexagonal CdSe nanoparticles exhibit a broad feature to the red of the band edge when capped with thiolate ligands, as shown in Figure 8. However, the process of oxidation-induced gelation actually decreases the band-edge peak relative to the trap peak, and the trap peak itself shows an increase in intensity at the blue end and a decrease at the red end, relative to the precursor nanoparticles. This suggests that more traps are present in the network

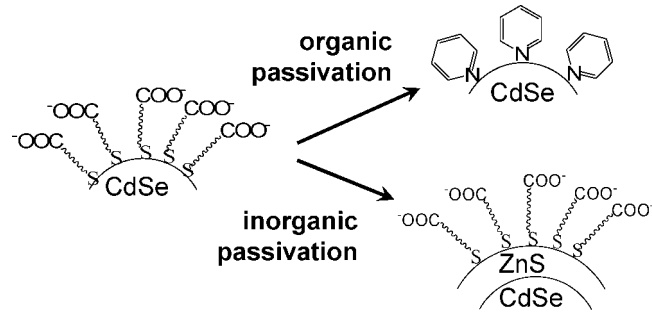

FIGURE 9. Scheme illustrating the approach to increasing the band-edge luminescence of CdSe gel networks by displacing thiolate groups bound at the CdSe surface that give rise to trap states. The thiolates can be exchanged with pyridine at the wet gel stage by solvent exchange. Alternatively, a coating of ZnS can passivate the CdSe surface.

structure and that the nature of the trap states is fundamentally different in these two materials. Is it then possible to recover or even improve upon the photoluminescence properties of the nanoparticle precursors within a gel architecture?

Surface passivation of semiconducting nanocrystals can minimize surface defects, thereby enhancing the possibility of emissive electron–hole recombination.[8] As illustrated in Figure 9, there are two main approaches: the derivatization of nanocrystals with surface-passivating ligands (organic passivation) or the growth of a second phase on the surface of the nanoparticle (inorganic passivation). Hence, we sought to apply these methods to metal chalcogenide gels with an eye toward increasing their emission properties.

With respect to organic surface passivation, we have tested the ability to remove residual thiolates (left from incomplete oxidation) from the nanostructure surface by ligand exchange with pyridine, because amines are known to be effective at reducing trap-state emission.[52] Energy-dispersive spectroscopic studies on thiolate-coated CdSe nanocrystals and derived gels have shown that sulfur from thiolates accounts for nearly 20 atom % of the precursor nanoparticles.[27] Upon gelation and aerogel formation, the sulfur content is reduced to 13–14 atom %, consistent with the oxidative removal of a portion of the surface thiolate groups concomitant with gelation. However, if the wet gels are exchanged with pyridine for several days prior to gel drying, we can further reduce the sulfur content of the gel network to approximately 6% by mole, because of the replacement of a portion of the residual thiolates with pyridine functionalities.[27] The consequence is a significant increase in the band-edge features of corresponding aerogels relative to the trap peak (Figure 8). In addition to improving the emission properties, this strategy also demonstrates that chemistry can still be done even after gelation and in a way that does not break up the nanoparticle network.

Inorganic passivation of the quantum dot by a wider band gap material is typically more effective at reducing trap-state emission (and thereby augmenting band-edge emission) than organic passivation techniques. Capping CdSe nanoparticles with a ZnS shell is a well-established

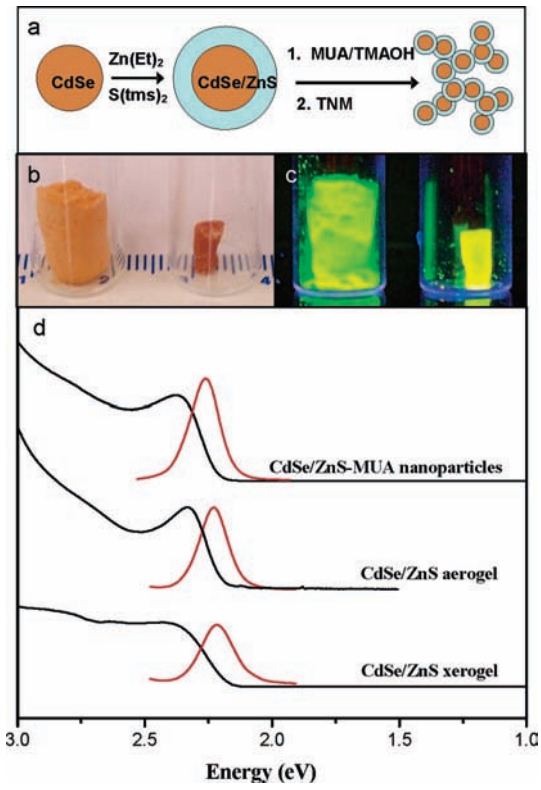

FIGURE 10. (a) Scheme showing the synthetic methodology for coating CdSe nanoparticles with ZnS shells by treatment with diethylzinc and tris(trimethylsilyl)sulfide and thiolate capping with MUA. By treatment with TNM, highly luminescent gels of CdSe/ZnS are formed, as shown in the photographs of corresponding aerogels (left monolith) and xerogels (right monolith) under (b) normal and (c) UV illumination. In d, the optical absorption (black) and photoluminescence (red) spectra of CdSe/ZnS core/shell nanoparticles, aerogels, and xerogels are presented. In contrast to gel structures prepared from bare CdSe, there is virtually no change in the band-edge energy among the different samples and the trap-state peak evident in Figure 7 is completely absent. Parts b–d of this figure were reproduced with permission from ref 53. Copyright 2007 American Chemical Society.

approach for preparing highly emissive quantum dots and has the further advantage that the shell is far more robust than most organic ligands (less susceptible to chemical exchange).[8] Therefore, we prepared CdSe/ZnS (core/shell) nanoparticles, capped them with thiolate (MUA), and linked them together via oxidation-induced gelation (Figure 10).[53] Monoliths can be prepared as both aerogels and xerogels and are highly emissive even when excited with a handheld UV lamp (Figure 10). Furthermore, in contrast to "naked" CdSe nanoparticle networks, the density of the network has very little influence on the optical and electronic properties of the core/shell nanostructures. Thus, both core shell aerogels and xerogels exhibit optical absorption and emission spectra that are essentially identical to those of the precursor nanoparticles (Figures 6 and 10). This is attributed to the ZnS barrier layer, which effectively reduces the interparticle interactions between core CdSe nanocrystals.

Conclusion and Outlook

The use of sol–gel methods for the assembly of metal chalcogenide quantum dots represents a powerful method for addressing a critical problem in the application of nanoparticles in technology: how to link particles together into purely inorganic 3D connected macrostructures while retaining the optoelectronic properties of the individual quantum dot. The simplicity of the method, which exploits established procedures for quantum dot synthesis and surface modification, and the generality of the approach to a wide range of metal chalcogenides, including sulfides and selenides of Zn, Cd, and Pb, suggest that it can be used routinely, as routinely as silica sol–gel methods! Because the quantum-confinement effects arise from the dimensionality of the network, the optical band gap can be tuned just by varying the density of the network. Additionally, organic or inorganic surface modification strategies originally developed for quantum dots can easily be applied to gels, enabling the characteristic luminescence properties of the dot to be retained in gels.

Quantum dot nanostructures are expected to address applications that individual quantum dots cannot. The combination of porosity and an interconnected nanoparticle network suggest they may be suitable when small molecule diffusion and large interfacial surface areas are needed, such as in sensing and photovoltaics. For example, the photoluminescence properties of CdSe quantum dots have been shown to be sensitive to Lewis bases, such as triethylamine, but the optical response of these materials is slow, because of diffusion problems.[54] In contrast, diffusion in aerogel structures has been shown to be similar to that in open air.[55] Likewise, CdSe nanoparticles have also been used in flexible photovoltaic devices by interfacing them to a hole-conducting polymer.[56] However, the device efficiencies are limited by the need for electron hopping between disparate nanoparticles. A prewired network, such as that present in the metal chalcogenide gel networks, should facilitate electron transport for such applications.

The application of sol–gel methods to metal chalcogenides, as well as previous work on carbon aerogels, suggests that perceived limitations on the chemistry accessible by sol–gel approaches are just that, *perceived*. Accordingly, we are now focused on extending non-oxide systems from sulfides and selenides to tellurides, such as CdTe and PbTe, as well as exploring the sol–gel chemistry of the Group 15 elements. Additionally, although the metal chalcogenide gels are morphologically identical to base-catalyzed silica gels, the nature of bonding between particles remains unknown. An investigation of the mechanism of gelation and the chemical nature of the bonding between nanoparticles in chalcogenide gel networks is currently underway.

We thank Mercouri Kanatzidis for the use of the solid-state optical band-gap equipment. The work summarized in this Account was supported in part by the National Science Foundation (CAREER, DMR-0094273; IGERT, DEG-9870720), Research Corporation (Research Innovation Award, R10617), and the donors

of the Petroleum Research Fund, administered by the American Chemical Society (43550-AC10). Electron microscopy was acquired at the Wayne State University (WSU) Central Instrumentation Facility on a JEOL 2010F, purchased under NSF Grant DMR-0216084.

References

(1) Afzaal, M.; O'Brien, P. Recent Developments in II–VI and III–VI Semiconductors and Their Applications in Solar Cells. *J. Mater. Chem.* **2006**, *16*, 1597–1602.

(2) Cai, W.; Shin, D.-W.; Gheysens, O.; Cao, Q.; Wang, S. X.; Gambhir, S. S.; Chen, X. Peptide-Labeled Near-Infrared Quantum Dots for Imaging Tumor Vasculature in Living Subjects. *Nano Lett.* **2006**, *6*, 669–676.

(3) Law, M.; Greene, L. E.; Johnson, J. C.; Saykally, R.; Yang, P. Nanowire Dye-Sensitized Solar Cells. *Nat. Mater.* **2005**, *4*, 455–459.

(4) Yan, H.; He, R.; Johnson, J.; Law, M.; Saykally, R.; Yang, P. Dendritic Nanowire Ultraviolet Laser Array. *J. Am. Chem. Soc.* **2003**, *125*, 4728–4729.

(5) Bruchez, M. P. Turning All the Lights On: Quantum Dots in Cellular Assays. *Curr. Opin. Chem. Biol.* **2005**, *9*, 533–537.

(6) Alivisatos, A. P. Semiconductor Clusters, Nanocrystals, and Quantum Dots. *Science* **1996**, *271*, 933–937.

(7) Scher, E. C.; Manna, L.; Alivasatos, A. P. Shape Control and Applications of Nanoparticles. *Philos. Trans. R. Soc. London, Ser. A* **2003**, *361*, 241–255.

(8) Trindale, T. O.; O'Brien, P.; Pickett, N. L. Nanocrystalline Semiconductors: Synthesis, Properties, and Perspectives. *Chem. Mater.* **2001**, *13*, 3843–3858.

(9) Shevchenko, E. V.; Talapin, D. V.; Kotov, N. A.; O'Brien, S.; Murray, C. B. Structural Diversity in Binary Nanoparticle Superlattices. *Nature* **2006**, *439*, 55–59.

(10) Shevchenko, E. V.; Talapin, D. V.; Murray, C. B.; O'Brien, S. Structural Characterization of Self-Assembled Multifunctional Binary Nanoparticle Superlattices. *J. Am. Chem. Soc.* **2006**, *128*, 3620–3637.

(11) Urban, J. J.; Talapin, D. V.; Shevchenko, E. V.; Murray, C. B. Self-Assembly of PbTe Quantum Dots into Nanocrystal Superlattices and Glassy Films. *J. Am. Chem. Soc.* **2006**, *128*, 3248–3255.

(12) Leunissen, M. E.; Christova, C. G.; Hynninen, A.-P.; Royall, C. P.; Campbell, A. I.; Imhof, A.; Dijkstra, M.; van Roij, R.; van Bladderen, A. Ionic Colloidal Crystals of Oppositely Charged Particles. *Nature* **2005**, *437*, 235–240.

(13) Springholz, G.; Holy, V.; Pinczolits, M.; Bauer, G. Self-Organized Growth of Three-Dimensional Quantum-Dot Crystals with fcc-Like Stacking and a Tunable Lattice Constant. *Science* **1998**, *282*, 734–737.

(14) Hoppe, K.; Geidel, E.; Weller, H.; Eychmüller, A. Covelently Bound CdTe Nanocrystals. *Phys. Chem. Chem. Phys.* **2002**, *4*, 1704–1706.

(15) Shavel, A.; Gaponik, N.; Eychmüller, A. The Assembly of Semiconductor Nanocrystals. *Eur. J. Inorg. Chem.* **2005**, 3613–3623.

(16) Wessels, J. M.; Nothofer, H.-G.; Ford, W. E.; von Wrochem, F.; Scholz, F.; Vossmeyer, T.; Schroedter, A.; Weller, H.; Yasuda, A. Optical and Electrical Properties of Three-Dimensional Interlinked Gold Nanoparticle Assemblies. *J. Am. Chem. Soc.* **2004**, *126*, 3349–3356.

(17) Brinker, C. J.; Scherer, G. W. *Sol–Gel Science*. Academic Press: San Diego, CA, 1990.

(18) Rolison, D. R.; Dunn, B. Electrically Conductive Oxide Aerogels: New Materials in Electrochemistry. *J. Mater. Chem.* **2001**, *11*, 963–980.

(19) Hüsing, N.; Schubert, U. Aerogels–Airy Materials: Chemistry, Structure, and Properties. *Angew. Chem., Int. Ed.* **1998**, *37*, 22–45.

(20) Pierre, A. C.; Pajonk, G. M. Chemistry of Aerogels and Their Applications. *Chem. Rev.* **2002**, *102*, 4243–4265.

(21) Brock, S. L.; Arachchige, I. U.; Kalebaila, K. K. Metal Chalcogenide Gels, Xerogels and Aerogels. *Comments Inorg. Chem.* **2006**, *27* (5–6), 1–24.

(22) Capoen, B.; Gacoin, T.; Nédélec, J. M.; Turrell, S.; Bouazaoui, M. Spectroscopic Investigation of CdS Nanoparticles in Sol–Gel Derived Polymeric Thin Films and Bulk Silica Matrices. *J. Mater. Sci.* **2001**, *36*, 2565–2570.

(23) Gacoin, T.; Lahlil, K.; Larregaray, P.; Boilot, J.-P. Transformation of CdS Colloids: Sols, Gels and Precipitates. *J. Phys. Chem. B* **2001**, *105*, 10228–10235.

(24) Gacoin, T.; Malier, L.; Boilot, J.-P. Sol–Gel Transition in CdS Colloids. *J. Mater. Chem.* **1997**, *7*, 859–860.

(25) Gacoin, T.; Malier, L.; Boilot, J.-P. New Transparent Chalcogenide Materials Using a Sol–Gel Process. *Chem. Mater.* **1997**, *9*, 1502–1504.

(26) Malier, L.; Boilot, J.-P.; Gacoin, T. Sulfide Gels and Films: Products of Non-oxide Gelation. *J. Sol-Gel Sci. Technol.* **1998**, *13*, 61–64.

(27) Arachchige, I. U.; Brock, S. L. Sol–Gel Assembly of CdSe Nanoparticles To Form Porous Aerogel Networks. *J. Am. Chem. Soc.* **2006**, *128*, 7964–7971.

(28) Arachchige, I. U.; Mohanan, J. L.; Brock, S. L. Sol–Gel Processing of Semiconducting Metal Chalcogenide Xerogels: Influence of Dimensionality on Quantum Confinement Effects in a Nanoparticle Network. *Chem. Mater.* **2005**, *17*, 6644–6650.

(29) Mohanan, J. L.; Arachchige, I. U.; Brock, S. L. Porous Semiconductor Chalcogenide Aerogels. *Science* **2005**, *307*, 397–400.

(30) Mohanan, J. L.; Brock, S. L. A New Addition to the Aerogel Community: Unsupported CdS Aerogels with Tunable Optical Properties. *J. Non-Cryst. Solids* **2004**, *350*, 1–8.

(31) Mohanan, J. L.; Brock, S. L. CdS Aerogels: Effect of Concentration and Primary Particle Size on Surface Area and Opto-electronic Properties. *J. Sol-Gel Sci. Technol.* **2006**, *40*, 341–350.

(32) Peng, Z. A.; Peng, X. Formation of High-Quality CdTe, CdSe, and CdS Nanocrystals Using CdO as Precursor. *J. Am. Chem. Soc.* **2001**, *123*, 183–184.

(33) Aldana, J.; Wang, Y. A.; Peng, X. Photochemical Instability of CdSe Nanocrystals Coated by Hydrophilic Thiols. *J. Am. Chem. Soc.* **2001**, *123*, 8844–8850.

(34) Kistler, S. S. Coherent Expanded Aerogels and Jellies. *Nature* **1931**, *127*, 741–741.

(35) Kistler, S. S. Coherent Expanded Aerogels. *J. Phys. Chem.* **1932**, *36*, 52–64.

(36) Gash, A. E.; Satcher, J. H., Jr.; Simpson, R. L. Strong Akaganeite Aerogel Monoliths Using Epoxides: Synthesis and Characterization. *Chem. Mater.* **2003**, *15*, 3268–3275.

(37) Gash, A. E.; Satcher, J. H., Jr.; Simpson, R. L. Monolithic Nickel(II)-Based Aerogels Using an Organic Epoxide: The Importance of the Counterion. *J. Non-Cryst. Solids* **2004**, *350*, 145–151.

(38) Kucheyev, S. O.; Baumann, T. F.; Cox, C. A.; Wang, Y. M.; Satcher, J. H., Jr.; Hamza, A. V.; Bradby, J. E. Nanoengineering Mechanically Robust Aerogels via Control of Foam Morphology. *Appl. Phys. Lett.* **2006**, *89*, 041911-1–3.

(39) Kucheyev, S. O.; Baumann, T. F.; Wang, Y. M.; van Buuren, T.; Poco, J. F.; Satcher, J. H., Jr.; Hamza, A. V. Monolithic, High Surface Area, Three-Dimensional GeO_2 Nanostructures. *Appl. Phys. Lett.* **2006**, *88*, 103117-1–3.

(40) Poco, J. F.; Satcher, J. H., Jr.; Hrubesh, L. W. Synthesis of High Porosity, Monolithic Alumina Aerogels. *J. Non-Cryst. Solids* **2001**, *285*, 57–63.

(41) Leventis, N.; Vassilaras, P.; Fabrizio, E. F.; Dass, A. Polymer Nanoencapsulated Rare Earth Aerogels: Chemically Complex but Stoichiometrically Similar Core–Shell Superstructures with Skeletal Properties of Pure Compounds. *J. Mater. Chem.* **2007**, *17*, 1502–1508.

(42) Gregg, S. J.; Sing, K. S. W. *Adsorption, Surface Area and Porosity*, 2nd ed.; Academic Press: New York, 1982.

(43) Webb, P. A.; Orr, C. *Analytical Methods in Fine Particle Technology*; Micromeritics: Norcross, GA, 1997.

(44) Yoffe, A. D. Low-Dimensional Systems: Quantum Size Effects and Electronic Properties of Semiconductor Microcrystallites (Zero-Dimensional Systems) and Some Quasi-Two-Dimensional Systems. *Adv. Phys.* **1993**, *42*, 173–266.

(45) Li, J.; Wang, L.-W. Band-Structure-Corrected Local Density Approximation Study of Semiconductor Quantum Dots and Wires. *Phys. Rev. B: Solid State* **2005**, *72*, 125325-1–15.

(46) Millo, O.; Steiner, D.; Katz, D.; Aharoni, A.; Kan, S.; Mokari, T.; Banin, U. Transition From Zero-Dimensional to One-Dimensional Behavior in InAs and CdSe Nanorods. *Physica E* **2005**, *26*, 1–8.

(47) Yu, H.; Li, J.; Loomis, R. A.; Gibbons, P. C.; Wang, L.-W.; Buhro, W. E. Cadmium Selenide Quantum Wires and the Transition from 3-D to 2-D Confinement. *J. Am. Chem. Soc.* **2003**, *125*, 16168–16169.

(48) Yu, H.; Li, J.; Loomis, R. A.; Wang, L.-W.; Buhro, W. E. Two- Versus Three-Dimensional Quantum Confinement in Indium Phosphide Wires and Dots. *Nat. Mater.* **2003**, *2*, 517–520.

(49) Emmerling, A.; Fricke, J. Small Angle X-ray Scattering and the Structure of Aerogels. *J. Non-Cryst. Solids* **1992**, *145*, 113–120.

(50) Bandaranayake, R. J.; Wen, G. W.; Lin, J. Y.; Jiang, H. X.; Sorensen, C. M. Structural Phase Behavior in II–VI Semiconductor Nanoparticles. *Appl. Phys. Lett.* **1995**, *67*, 831–833.

(51) Murray, C. B.; Norris, D. J.; Bawendi, M. G. Synthesis and Characterization of Nearly Monodisperse CdE (E = S, Se, Te) Semiconductor Nanocrystallites. *J. Am. Chem. Soc.* **1993**, *115*, 8706–8715.

(52) Bullen, C.; Mulvaney, P. The Effects of Chemisorption on the Luminescence of CdSe Quantum Dots. *Langmuir* **2006**, *22*, 3007–3013.

(53) Arachchige, I. U.; Brock, S. L. Highly Luminescent Quantum Dot Monoliths. *J. Am. Chem. Soc.* **2007**, *129*, 1840–1841.

(54) Nazzal, A. Y.; Lianhua, Q.; Peng, X.; Xiao, M. Photoactivated CdSe Nanocrystals as Nanosensors for Gas. *Nano Lett.* **2003**, *3*, 819–822.
(55) Leventis, N.; Elder, I. A.; Rolison, D. R.; Anderson, M. L.; Merzbacher, C. I. Durable Modification of Silica Aerogel Monoliths with Fluorescent 2,7 Diazapyrenium Moieties. Sensing Oxygen near the Speed of Open-Air Diffusion. *Chem. Mater.* **1999**, *11*, 2837–2845.
(56) Huynh, W. U.; Dittmer, J. J.; Alivisatos, A. P. Hybrid Nanorod–Polymer Solar Cells. *Science* **2002**, *295*, 2425–2427.

AR600028S